Special Issue Article

Institution of MECHANICAL ENGINEERS
Journal of ENGINEERING TRIBOLOGY

Proc IMechE Part J:
J Engineering Tribology
226(6) 481–500

DOI: 10.1177/1350650111431790
pij.sagepub.com
SAGE

Fluid rheology, traction/creep relationships and friction in machine elements with rolling contacts

GWG Poll and D Wang

Abstract

The correct prediction of shear stresses in lubricants applied to concentrated rolling/sliding contacts has been an issue of intense debate for many years. Traction testers of various kinds such as two-disc roller rigs or ball on disc apparatus have been extensively used in order to obtain experimental data, as well as, more recently, molecular dynamics simulations. Several, partly competing, phenomenological models have been developed to describe the dependence of shear stresses on various parameters. Evidently, the importance lies in the need to predict and reduce friction, or, more accurately, resistance to motion of rolling element bearings in order to increase efficiency of machines and vehicles. Also, it plays a crucial role in design and performance of traction drives. As a prerequisite, experimental data for a wide variety of fluids were obtained from two-disc roller tests with a wide variation of contact pressures, rolling speeds and slide-to-roll ratios. Following earlier investigations, the amount of slip created by the elastic deformation of the discs was separated from the contribution of the fluids and their rheological properties. In accordance with experiments of Jacobson a threshold pressure in the fluid was identified which marks the onset of a nearly linear relationship between a limiting shear stress and pressure. However, this threshold does not appear to be constant but rather declining with decreasing hydrodynamic film thickness respective of rolling speed, while the slope changes to a lesser extent. When measurements were extended far into the mixed lubrication regime close to the limiting case of boundary lubrication, the shear stress/pressure relationship became quasi-Coulomb with a virtually zero threshold pressure. These results have successfully been used to predict the friction torque of angular contact ball bearings and the traction characteristics in toroidal drives.

Keywords

Lubricant rheology, rolling contacts, traction–creep relationship, limiting shear stress, viscoelasticity

Date received: 7 September 2011; accepted: 24 October 2011

Introduction

The rheology of lubricating fluids has been studied for a long time, but there are still some aspects which continue to be subject to debate. In the study of Bair and Kotzalas,[1,2] two of those are addressed:

(a) the existence and nature of a limiting shear stress;
(b) the determination of the elastic modulus of fluids.

Especially, there are still questions how to interpret traction–creep curves measured at roller test machines with respect to basic rheological properties of the investigated fluids.

In this article, traction measurements involving a wide range of parameter variations at a two-disc roller test rig are re-evaluated with the aim to promote the ongoing discussion.

Figure 1 shows typical traction measurements with a two-disc roller test machine (Figure 2). Figure 1(a) and (b) shows the mean Hertzian contact pressure and the rolling speed, respectively, which are the varied parameters, while the oil inlet temperature is controlled to be a constant 60°C.

Institute of Machine Elements, Engineering Design and Tribology (IMKT), Leibniz Universitaet Hannover, Germany

Corresponding author:
GWG Poll, Institute of Machine Elements, Engineering Design and Tribology (IMKT), Leibniz Universitaet Hannover, Welfengarten 1A, Hannover D-30167, Germany.
Email: poll@imkt.uni-hannover.de

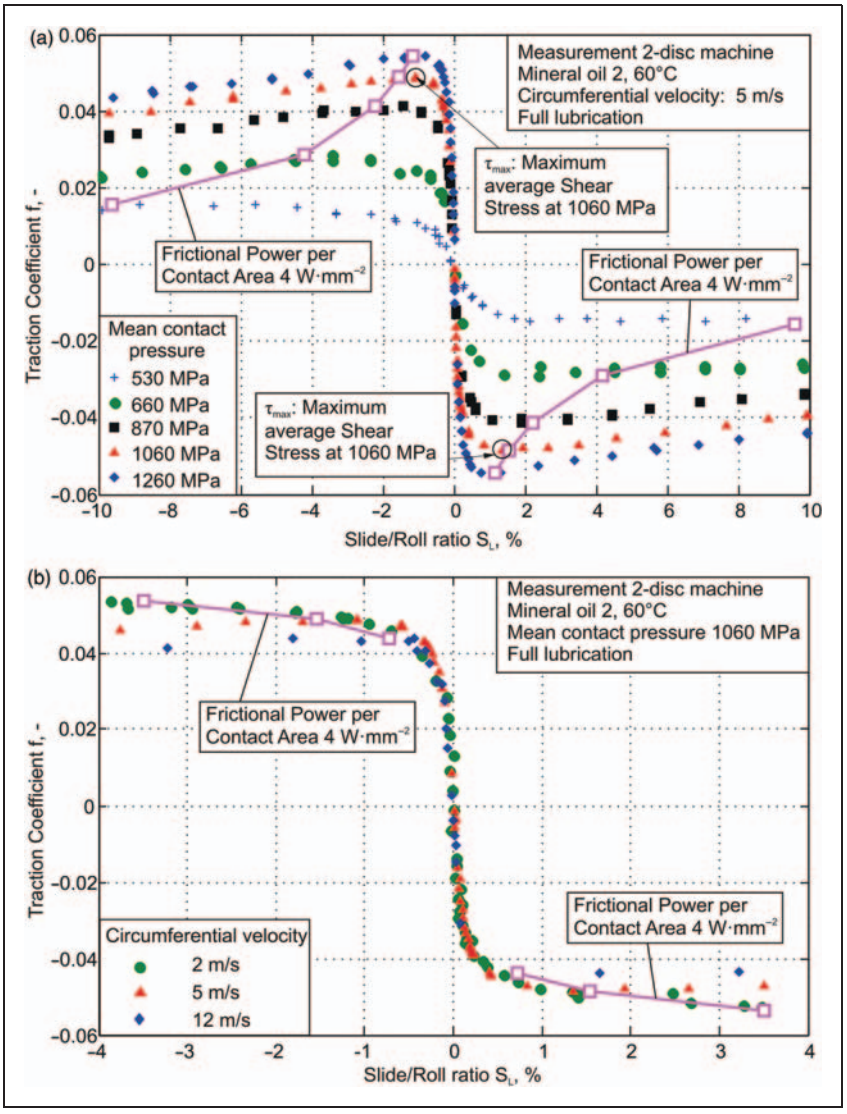

Figure 1. Traction coefficients plotted versus slide-to-roll ratio measured on the two-disc roller rig at Hannover University for (a) different average contact pressures[3,4] and (b) different rolling speeds.[4]

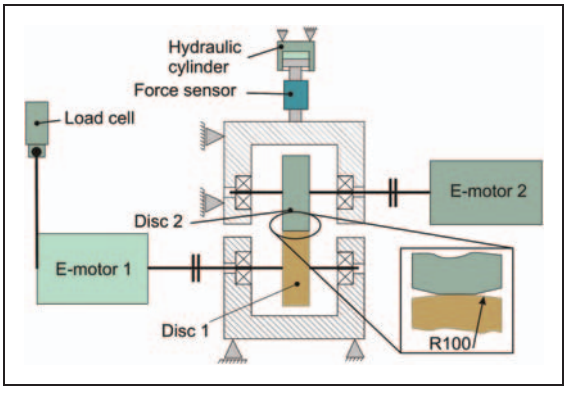

Figure 2. Two-disc roller rig at Hannover University used for the traction measurements in Figure 1.[4]

The oil is directly fed into the contact via a nozzle with a thermal sensor incorporated. Almost identical results were already obtained by Plint[5] as early as 1967 and analysed in detail by Johnson and Cameron[6] and Dyson.[7]

The degressive trend of the curves with an almost linear region close to the origin and a levelling out, a plateau or a pronounced maximum and a subsequent decline at high slip values may be interpreted as an Eyring type[8] shear rate-dependent viscous behaviour

$$\dot{\gamma} = \frac{\tau_0}{\eta} \cdot \sinh\left(\frac{\tau}{\tau_0}\right) \tag{1}$$

the superimposition of an elastic contribution to shear[9]

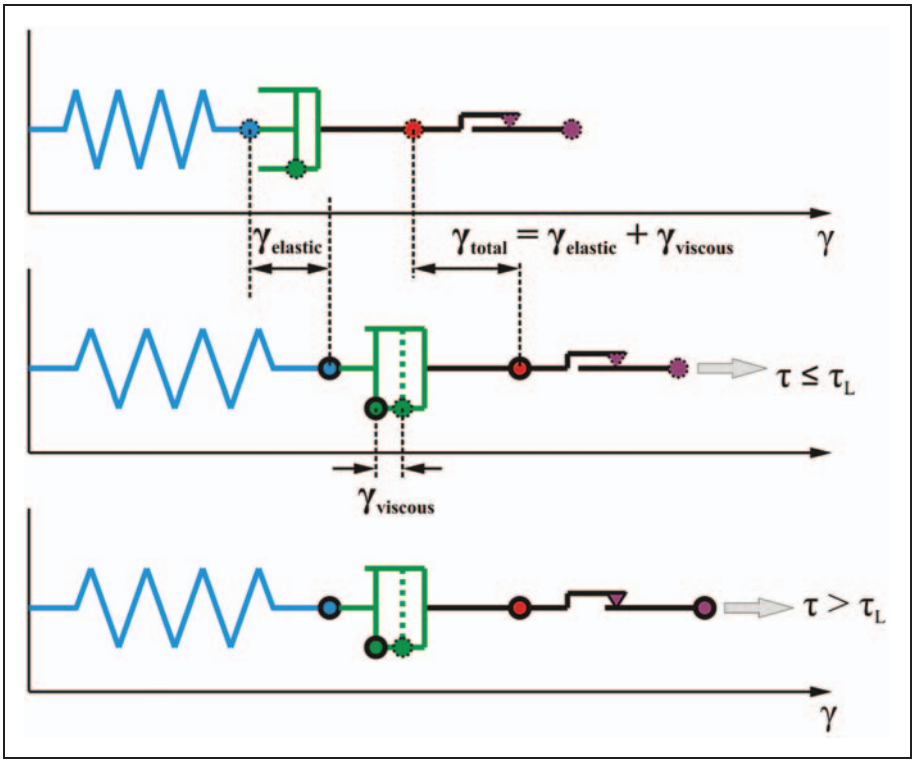

Figure 3. Maxwell model of a visco-elastic fluid with limiting shear stress.

$$\dot{\gamma} = \frac{1}{G} \cdot \frac{\mathrm{d}\tau}{dt} + \frac{\tau_0}{\eta} \cdot \sinh\left(\frac{\tau}{\tau_0}\right) \tag{2}$$

or the additional introduction of a limiting shear stress[10]

$$\dot{\gamma} = \frac{1}{G_\infty} \cdot \frac{\mathrm{d}\tau}{dt} + \frac{\tau_L}{\eta} \cdot \ln\left(\left(1 - \frac{\tau}{\tau_L}\right)^{-1}\right) \tag{3}$$

The latter equation describes a Maxwell model with an in-line arrangement of three elements: a spring, a viscous dashpot and a damper with 'dry' friction (Figure 3). It is also known as the Bair–Winer model.

There are a number of other possible equations given in the study of Bair and Winer[10] and it should be noticed that these approaches mainly attempt to approximately describe experimental results in combination with more or less hypothetical physical models.

It is interesting to note that for dry rolling contacts, curves similar to Figure 1 may be obtained and, according to the theoretical approach of Carter[11] which gave the first exact solution for pure line contacts, can be described by

$$S_L(f) = 2 \cdot f \cdot \bar{p} \cdot \frac{1-\nu}{G} \cdot \frac{\pi}{4} \cdot \left(1 - \sqrt{1 - \frac{f}{f_{\max}}}\right) \tag{4}$$

In this case, slip or creep originates from the elastic deformation of the contacting bodies. When Coulomb friction prevails, the coefficient of sliding friction $f_{\max}$ represents an upper limit to traction very much like a limiting shear stress in lubricated contacts. Coulomb's law in fact describes the limiting case where the maximum shear stress during sliding is strictly proportional to contact pressure. Therefore, an initially linear region of the traction curve around the origin has to be followed by a non-linear transition to sliding with a constant coefficient of friction. During the transition, there is a growing area of slip in the contact area where the limiting shear stress is reached (Figure 4). A contact lubricated by a fluid with purely elastic properties and a limiting shear stress strictly proportional to pressure would yield the same traction characteristics as a dry contact of solid bodies. It can simply be regarded as an elastic layer on top of the solid rolling elements (Figure 5).

However, in contrast to Coulomb-type solid friction, in the case of a lubricant film, viscous relaxation substantially alters the shear stresses related to a specific amount of shear. Hence, the maximum traction shifts to higher slip values. Higher rolling speeds and therefore shorter passage times through the contact principally reduce the effect of relaxation. Therefore, in contrast to dry contacts with Coulomb type friction, there will be an influence of rolling speed.

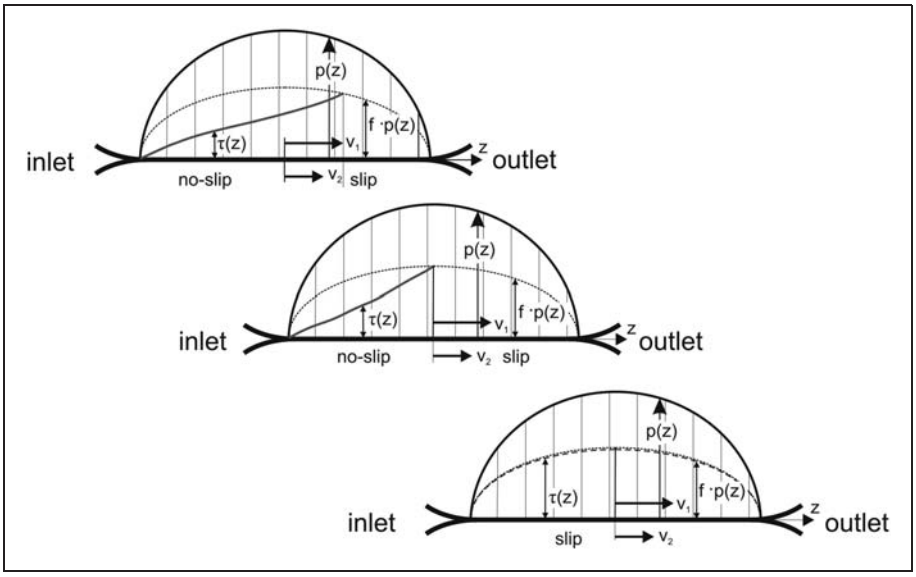

Figure 4. Distribution of shear stresses, no-slip and slip zones in a dry rolling contact; total slip and traction increasing from top to bottom according to Carter[11] and Poll.[12]

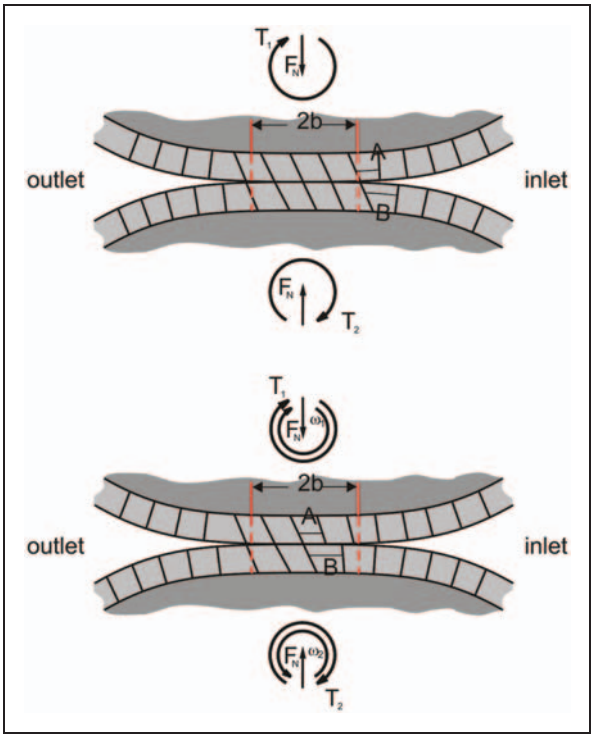

Figure 5. Shear deformation of layers when passing through a rolling contact with slip.[12]

Thermal effects are present in solid contact, boundary and full film lubrication to a different extent, but generally tend to reduce friction at elevated sliding velocities. Therefore, there should be always a maximum of traction rather than a true plateau representing the isothermal limiting shear stress, provided one reaches sufficiently high sliding velocities. This is indicated in Figure 1 with curves representing a constant frictional loss per unit contact area. The traction maxima or, in other words, the onset of decline of traction always occur around a value of $4\,W/mm^2$. Given the *Peclet* numbers involved, heat transfer via the contact surfaces into the adjacent solid bodies may be assumed to prevail and, therefore, a similar frictional loss per unit contact area indicates similar temperatures in the contact. The negative slope of traction curves beyond the maximum is therefore confirmed to be a thermal effect, as described among others in the study of Olver and Spikes[13] and Tevaarwerk.[14]

In order to extract the information regarding the rheological properties of the fluid, the contribution of the contacting solid bodies to slip has to be subtracted, as proposed by Bair following a discussion with the author of this article.[1] However, to do so, very accurate measurements are required and, sometimes, as with fluids investigated in the study of Bair and Kotzalas,[1] it appears as if there is no elastic contribution of the fluid at all and the tangent of the traction curve at the origin is merely due to the elastic deformation of the contacting bodies.

An additional effect which may be of great influence when evaluating different speeds and temperatures is a possible transition from full film lubrication to mixed or even boundary lubrication due the variation of film thickness. In case one wants to determine the elastic modulus G_∞, the rolling speeds should be high and therefore film thicknesses will be high. In case one

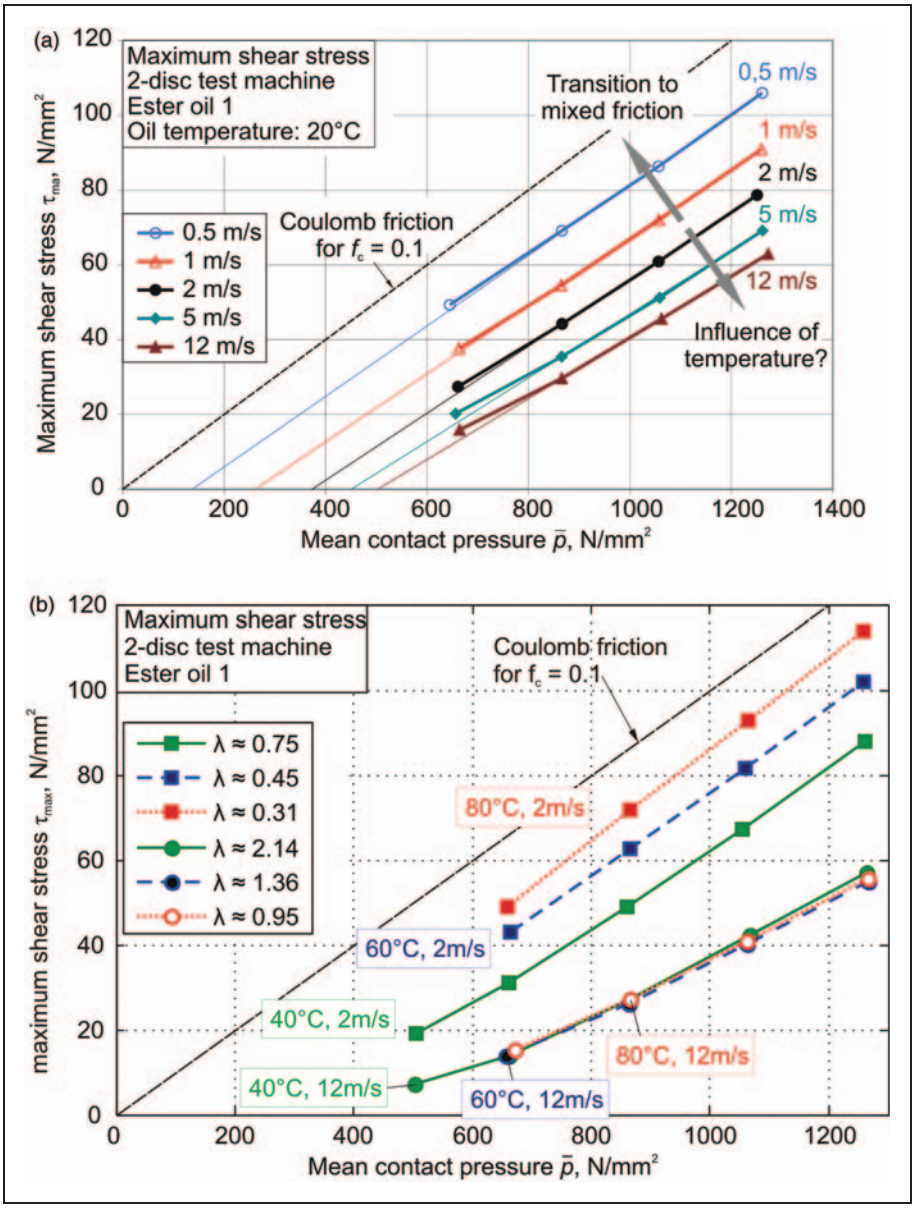

Figure 6. Maximum average shear stresses in the contact zone plotted against mean Hertzian pressure for ester oil 1 at different rolling speeds and at (a) 20°C[3,4] and (b) other temperatures.

Table 1. Properties of the experimental fluids.

Lubricant	Oil 1	Oil 2
Oil type	Ester	Mineral
Oil viscosity at 40°C $\nu_{40°C}$ (mm/s²)	23	280
Oil viscosity at 100°C $\nu_{100°C}$ (mm/s²)	4.7	22

wants to study viscosity and reduce the influence of elasticity by increasing relaxation time, one prefers very low speeds which lead to thinner films. Then, the maximum or possibly limiting shear stress may partly be due to Coulomb type boundary friction and the λ ratio of fluid film thickness to roughness has to be carefully observed.

One interpretation of measurements is to assume strict proportionality between pressure and limiting shear stress, that means an almost linear relation which passes through the origin.[15] Others, like Bair[10] and Jacobson[16] also report measurements where the linear increase starts from a threshold value of pressure. This leads to the question if the extrapolation of measurements through the origin found in literature is always correct.

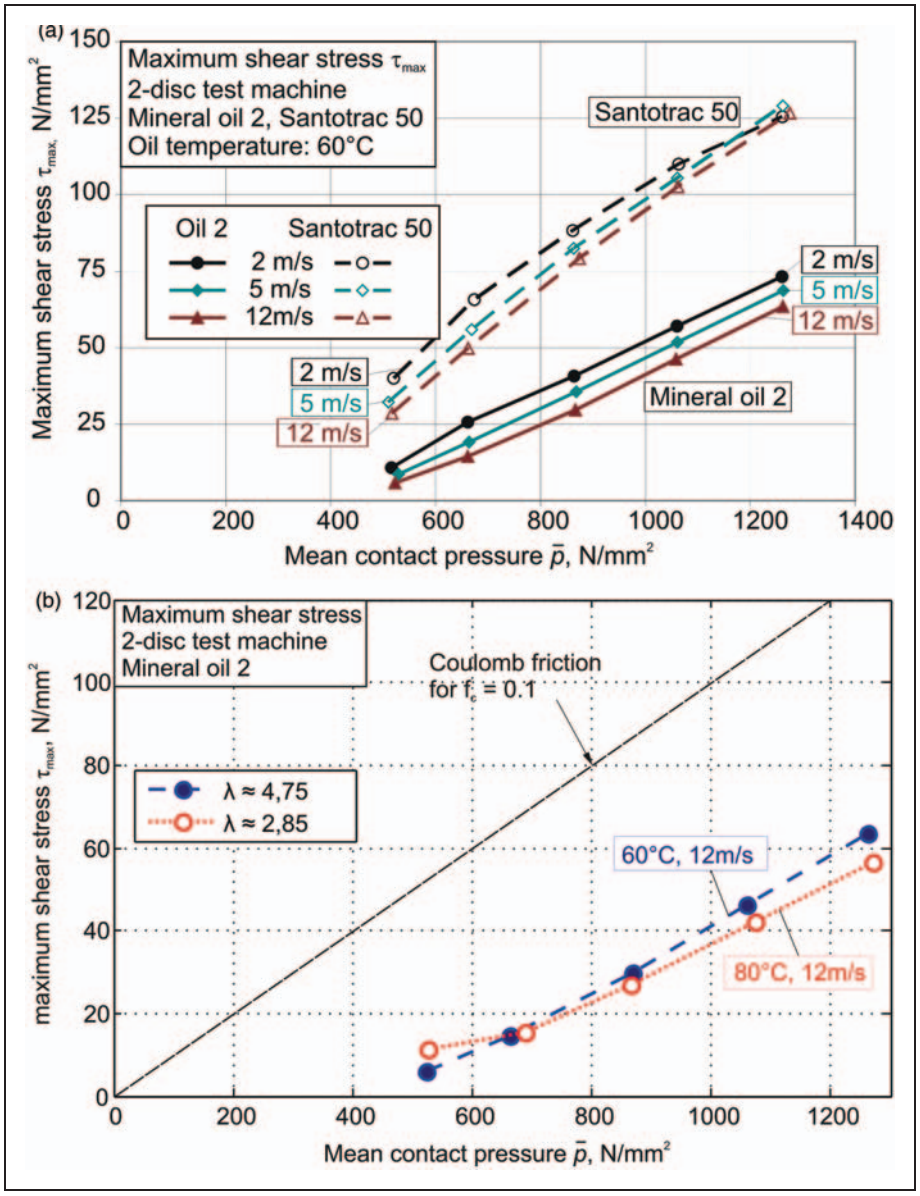

Figure 7. Maximum average shear stresses in the contact zone plotted against mean Hertzian pressure for mineral oil 2 at 60°C oil inlet temperature/different rolling speeds compared to (a) *Santotrac 50*[3] and 60, respectively 80°C oil inlet temperatures/12 m/s rolling speed (b).

The following evaluations start from the hypothesis that the assumptions underlying the Bair–Winer model hold true. The objective was to check if the measured behaviour could be reproduced on the basis of this hypothesis and its implications, especially:

(a) there is a limiting shear stress;
(b) the shear of the lubricant in the EHD-film is partly elastic, partly viscous.

These two aspects will be separately addressed in the following paragraphs.

Limiting shear stress

The easiest way to derive approximate values for postulated limiting shear stresses from measured traction curves in rolling contact is to evaluate the maximum traction coefficients determined for different Hertzian pressures, rolling speeds and oil inlet temperatures (Figure 1).

By relating the corresponding resulting tangential forces to the respective Hertzian contact areas, one obtains a mean shear stress for the contact, or one

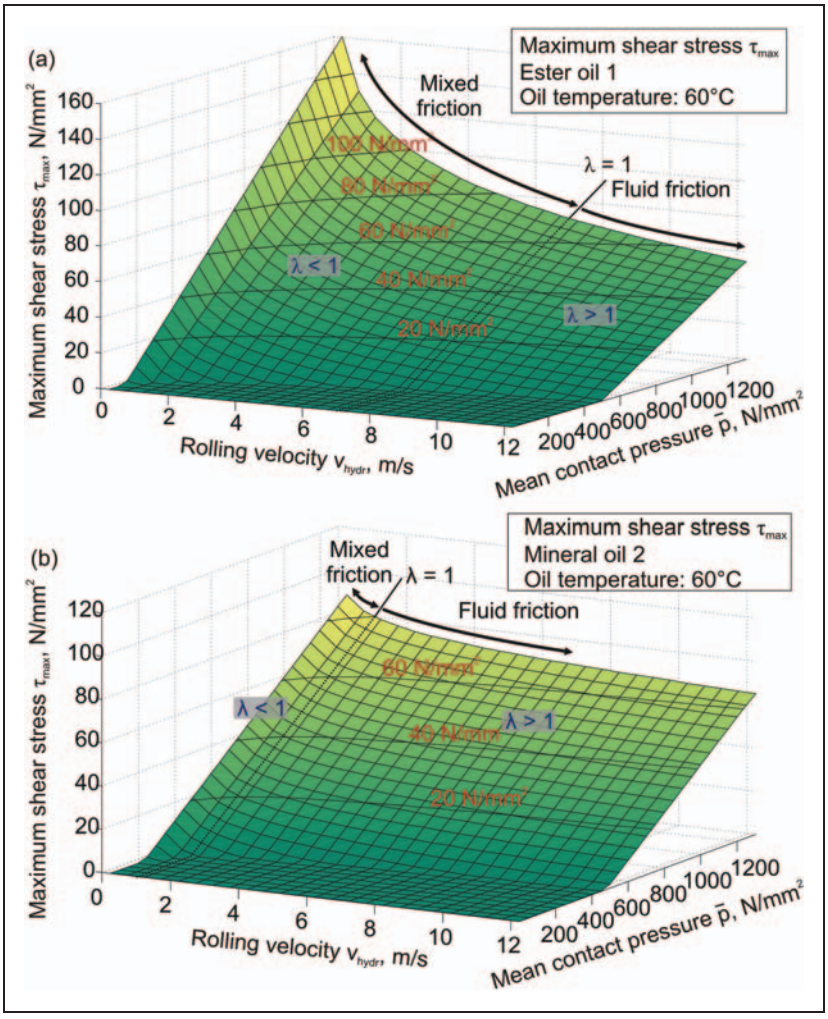

Figure 8. Maximum average shear stresses in the contact zone (oil inlet temperature 60°C) plotted in a 3D map for (a) ester oil 1[3] and (b) mineral oil 2.[3,4]

may also multiply the mean Hertzian pressure with the traction coefficient

$$\bar{\tau} = \frac{F_t}{\pi \cdot a \cdot b} = \bar{p} \cdot f \tag{5}$$

and therefore

$$\bar{\tau}_L(\bar{p}, v, \theta) = \bar{p} \cdot f_{\max}(\bar{p}, v, \theta) \tag{6}$$

Consequently, it should then be plotted versus the mean Hertzian pressure (Figures 6 and 7). This averaging approach is a first approximation, as it would only represent the exact correlation between limiting shear stress and pressure in case there would be a strict proportionality between pressure and shear stress throughout the contact. Also, as mentioned before, it is not possible to measure isothermal limiting shear stresses.

However, as the evaluated maxima are all roughly subject to the same frictional heating, the resulting plots at least represent maximum average shear stresses at a fairly constant average contact temperature. Therefore, the experimentally determined maximum average shear stresses are subsequently simply addressed as limiting shear stresses. On the other hand, there are important variations of film thickness as a result of the purposely varied speeds and oil inlet temperatures and therefore, the λ ratios are indicated as well. Here, the classic formula for λ is used

$$\lambda = \frac{h_c}{\sqrt{\sigma_1^2 + \sigma_2^2}} \tag{7}$$

$$\sigma_{1,2} = \sqrt{\frac{\pi}{2}} \cdot R_{a1,2} \tag{8}$$

Figure 6 was obtained with the ester oil 1 (Table 1). Figure 7 originated from measurements with the

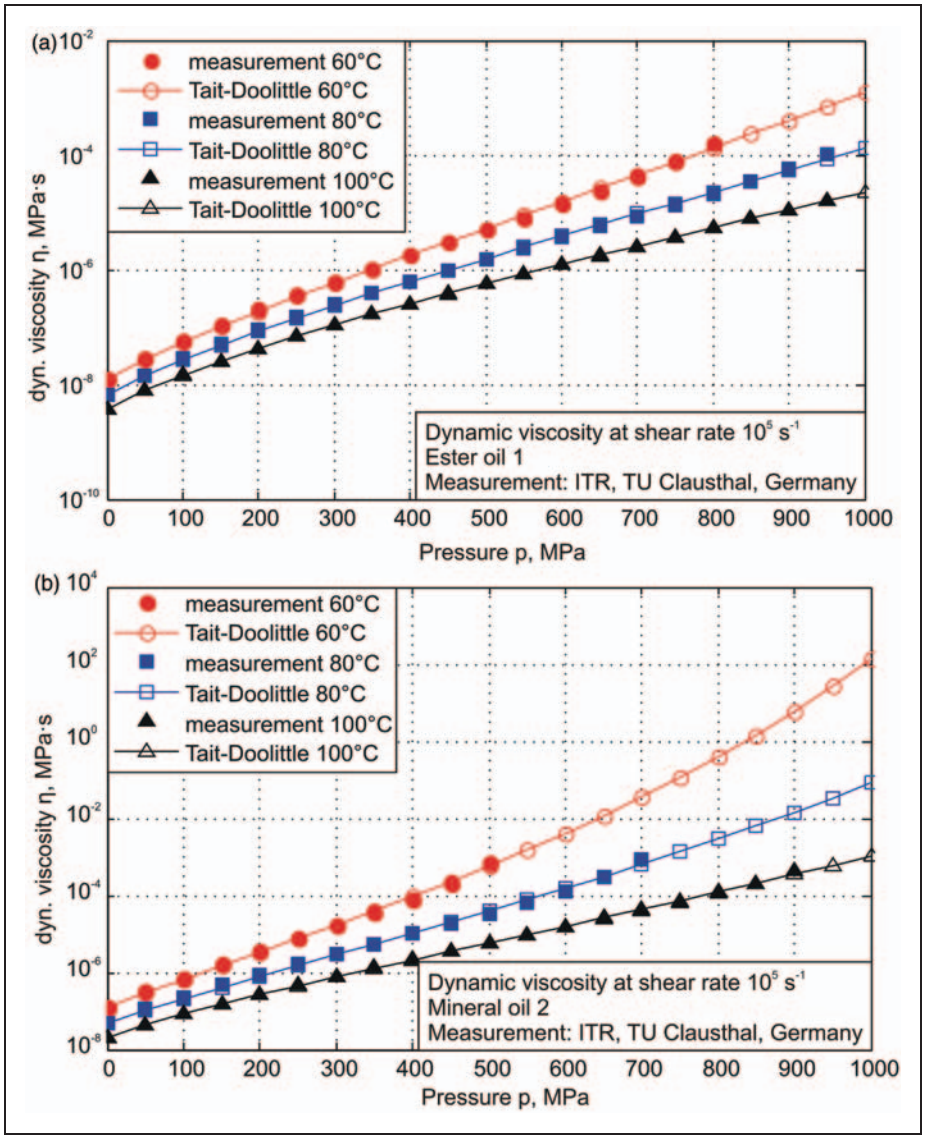

Figure 9. Viscosity measurements with an oscillating quartz instrument under pressures from 0 to 1 GPa and temperatures from 60 to 100°C at a mean shear rate of $10^5 00A0 s^{-1}$, fitted with Tait–Doolittle model[19,20] for (a) ester oil 1[4] and (b) mineral oil 2.

mineral oil 2. For a better understanding, the same results can also be represented with 3D plots like in Figure 8.

The central film thickness is calculated according to Hamrock and Dowson.[17] The viscosity values were determined in an oscillating quartz rheometer[18] at the Institute of Tribology and Energy Conversion Machinery at the Technical University of Clausthal (Figure 9). The mean shear rates were selected to be well within the range occurring in the evaluated experimental investigations. The 'S-shape' of the curves is a characteristic of glass forming liquids and in line with the free volume theory.[18] It may be described according to Tait–Doolittle.[19,20]

From these measurements, pressure viscosity coefficients were derived based on the Barus approach[21] for 200 MPa (2000 bar) pressure

$$\eta(p,\theta) = \eta_0(\theta) \cdot e^{\alpha_{p2000}(\theta)\cdot p} \tag{9}$$

$$\alpha_{p,2000}(\theta) = \frac{\ln(\eta_1(p_1,\theta)) - \ln(\eta_0(p_0,\theta))}{p_1 - p_0} \tag{10}$$

with $p_1 = 200$ MPa, and $p_0 = 0.1$ MPa.

This is not in line with the original proposal of Hamrock and Dowson but has later been shown by Walbeck[22] to result in a good approximation of experimental values of film thickness as the inlet

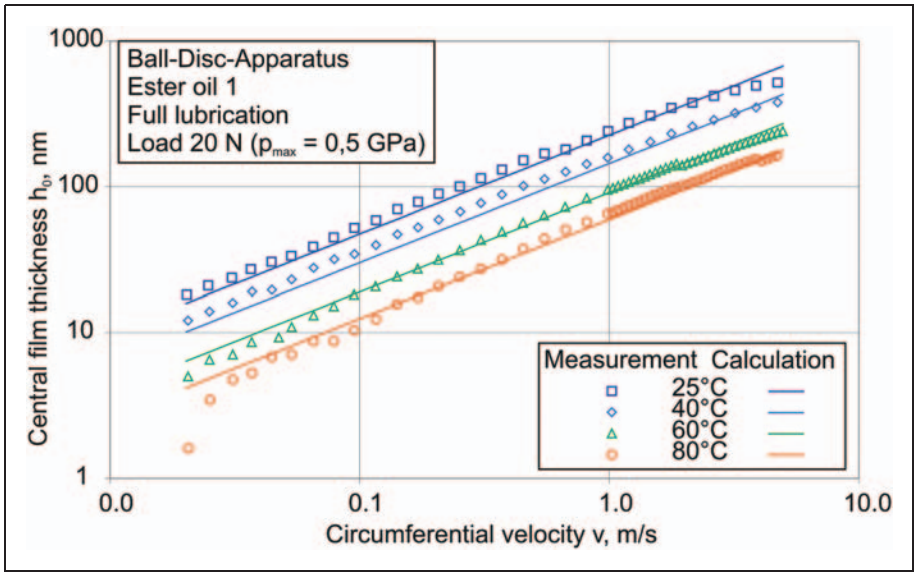

Figure 10. Interferometric measurements of central film thickness of ester oil 1 at different temperatures with a ball on disc apparatus and corresponding calculations according to Hamrock and Dowson using $\alpha_{p,2000}$ values.[4]

region with its moderate pressures dominates film formation. This is confirmed by interferometric film thickness measurements with a ball-on-disc apparatus (Figure 10).

As a conclusion, the experimental evidence does not discredit the concept of limiting shear stress. The relationship with pressure found here is principally in accordance with the Mohr–Coulomb failure criterion,[23] indicating the formation of shear bands.[24] However, according to the evaluations in this article, the limiting shear stresses would not be strictly proportional to pressure, but rise almost linearly beyond a pressure threshold value. The threshold value would then decrease with rolling speed as well as with temperature, as long as full film lubrication prevails. As similar, but not exactly equal, contact temperatures at the traction maximum may be assumed for all speeds, it is not certain if the influence of speed is thermal, too, or an effect in its own right possibly related to transit times through the contact or film thickness. When entering the mixed lubrication regime around $\lambda = 1$, the threshold values will rapidly decrease until a quasi-Coulomb relationship with a strict proportionality between maximum shear stress and mean pressure is reached at very low λ ratios at the transition from mixed to boundary lubrication. This happens through a reduction in rolling speed as well as through a continued increase in temperature. In Figure 6(b), at 2 m/s, this effect of temperature is clearly visible as the thinner ester oil 1 does not allow for full film lubrication. At 12 m/s, there is a reversal of the trend when increasing the temperature beyond 60°C as this encompasses a transition from full film into mixed lubrication. In Figure 7(b), for the mineral oil 2 with higher viscosity, the same temperature increase clearly reduces shear stresses as full film lubrication continues to prevail. In Figure 7(a), measurements with the well-known traction fluid *Santotrac 50* are included which show a behaviour qualitatively very similar to the mineral oil 1, albeit with a lower threshold value and a steeper slope.

Once again, it should be noted that the limiting shear stress values derived here are the results of an averaging across the contact and, therefore, do not truly correspond to the respective pressures, except for the high pressure range where the portion of the contact zone with pressures below the threshold may be negligibly small. At low and medium contact pressures, there will be substantial parts of the contact where the local shear stresses do not follow the linear limiting shear stress relationship and this will be reflected by the averaged values.

More insight can be gained by analysing the complete trend of the measured traction curves. However, for this purpose, one needs to define the other parameters in formula (3), which are elastic modulus and viscosity. Viscosity depends on pressure in a strongly non-linear way, which, together with the near Hertzian pressure distribution in the film, leads to extreme viscosity variations. Averaging across the contact can therefore not be used to identify the true viscous properties of the lubricant. Moreover, as the critical shear stress which limits Newtonian behaviour is easily exceeded at the pressures applied in the

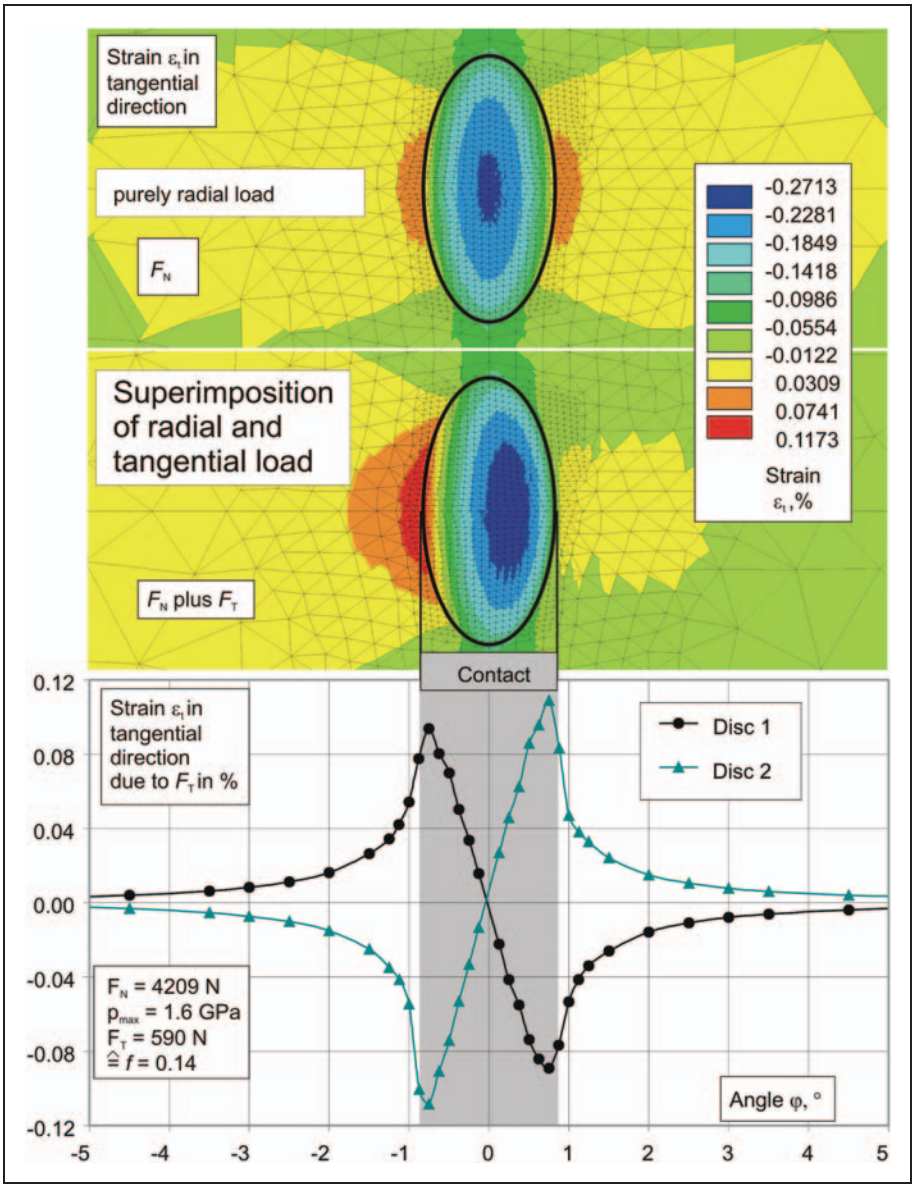

Figure 11. Longitudinal elastic strains at the surface in the vicinity of the contact due to tangential traction, FE-calculation with no-slip restraint.[4]

evaluated measurements, shear thinning will certainly occur, although partly being obscured by the dominance of the limiting shear stresses. Therefore, instead of one viscosity value for a given pressure and temperature, viscosity would depend on shear rate according to the Carreau equation.[25] Even the initial slope of the traction curve may seem to change as a result, because the critical shear stress for the transition to non-Newtonian behaviour is in the range of 5 MPa and will be exceeded already at very small slide-to-roll ratios. Therefore, using the averaging approach without considering the local shear stresses based on physical models and laboratory measurements, one can only derive 'equivalent' or 'effective' rheological parameters fitted to make the Bair–Winer model match the measured data.

Characterisation of viscoelastic properties

The analysis of traction curves in the vicinity of the origin principally allows to study the influence of viscous and elastic fluid properties almost independently from the questions concerning the limiting shear stress and frictional heating. However, as pointed out before, it is hard to escape from the effects of shear thinning. The measured data for 1 GPa average Hertzian contact pressure in Figure 1 were in a first step stripped of the portion of slip contributed by the elastic deformation of

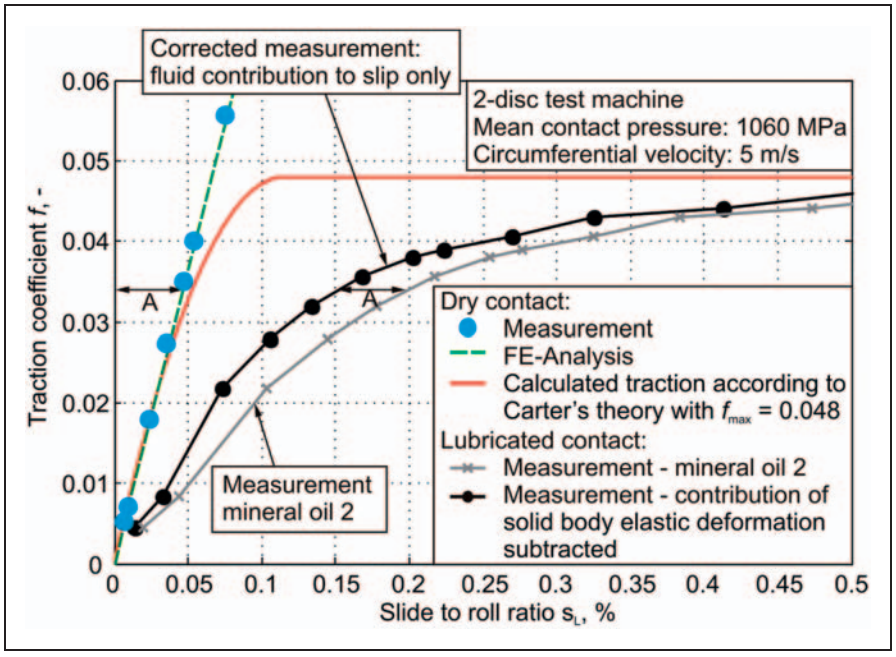

Figure 12. Determination of the fluid contribution to slip for mineral oil 2.[4]

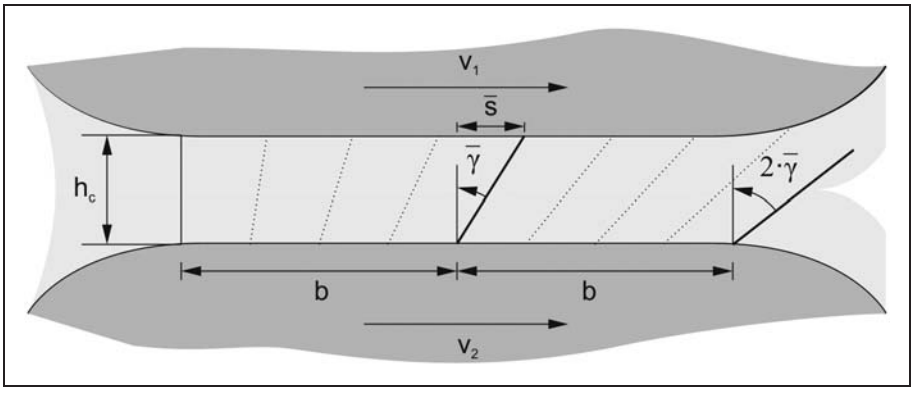

Figure 13. Build-up of shear in the fluid film in the direction of rolling.[4]

the contacting solid bodies in order to obtain the true relationship for the fluid itself. For that purpose, two methods were applied and compared. The experimental approach was to experimentally determine the slope at the origin by carefully cleaning the surfaces and measure traction and slip in the vicinity of the origin in dry conditions. Because the maximum coefficient of friction in dry condition exceeds 0.15, traction is practically proportional to slip in the range investigated. Then, the elastic strains at the surface of the discs were determined using a finite element model (FEM) of the two discs with an appropriate discretisation in the contact zone. As in this case only the linear behaviour at very small slip values is of interest, the onset of a sliding zone at the trailing edge of the contact can be neglected and no relative motion was allowed between the surface elements. One way to determine slip is then to add the amounts of the tangential surface strains caused by traction at the inlet of the contact area (Figure 11)

$$S_L = \left|\varepsilon_{T,1}\right| + \left|\varepsilon_{T,2}\right| \tag{11}$$

Figure 12 shows the excellent match of experimental and FEM results showing that the elastic deformations of the solid bodies substantially contribute to overall slip. Subsequently, the measured curves with combined slip are transformed into the curves of fluid slip by subtracting the elastic solid body slip 'A' contributed by the rollers (Figure 12). The theoretical traction curve

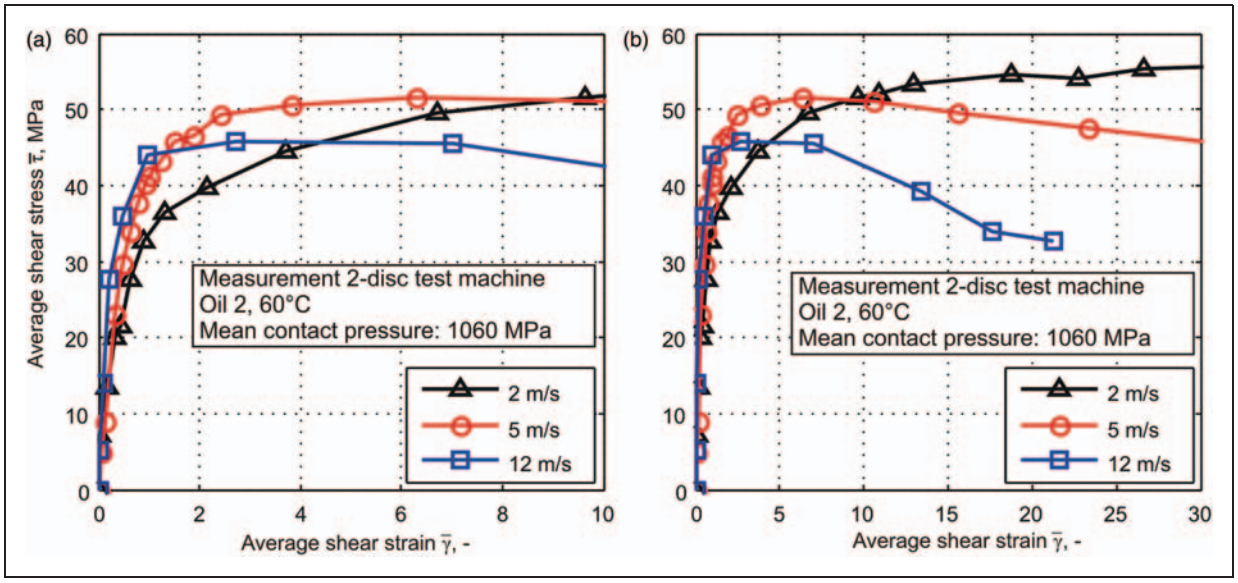

Figure 14. Average shear stress plotted against average shear strain at different circumferential velocities for mineral oil 2 in (a) vicinity of origin and (b) full range.

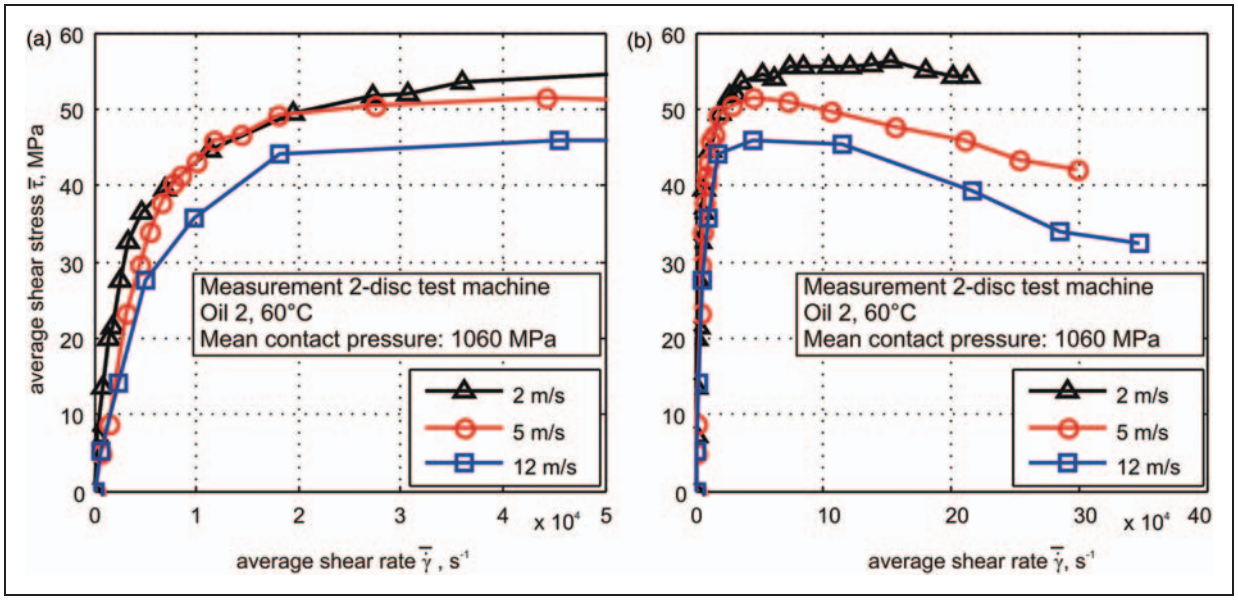

Figure 15. Average shear stress plotted against average shear rate at different circumferential velocities for mineral oil 2^4 in (a) vicinity of origin and (b) full range.

for a dry contact and Coulomb-type friction according to Carter[11] is indicated as well. The Coulomb friction coefficient f_{max} was chosen equal to the maximum traction coefficient found in lubricated condition. The discrepancy between dry and lubricated traction curves clearly indicates the viscoelastic contribution of the fluid. It should be noted that, in contrast to the fluid contribution, the slip produced by the elastic deformation of the rolling elements is completely independent of rolling speed and therefore only needs to be determined once for a given normal load and contact geometry. The curves representing fluid behaviour are then further transformed by calculating average shear values and shear rates by relating the tangential displacement of the walls given by slip to the central film thicknesses

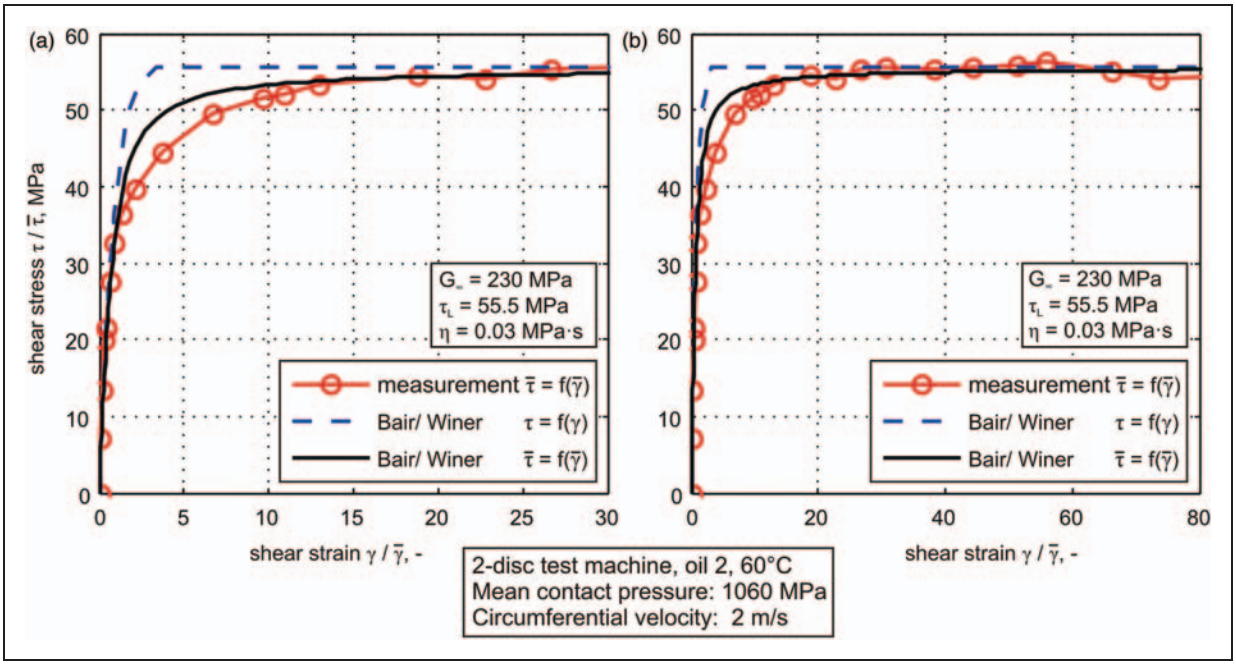

Figure 16. Comparison between experimental results and calculations of shear stress for mineral oil 2 by applying the Bair–Winer model against both shear and average shear strains at a rolling speed of 2 m/s in (a) vicinity of origin and (b) full range.

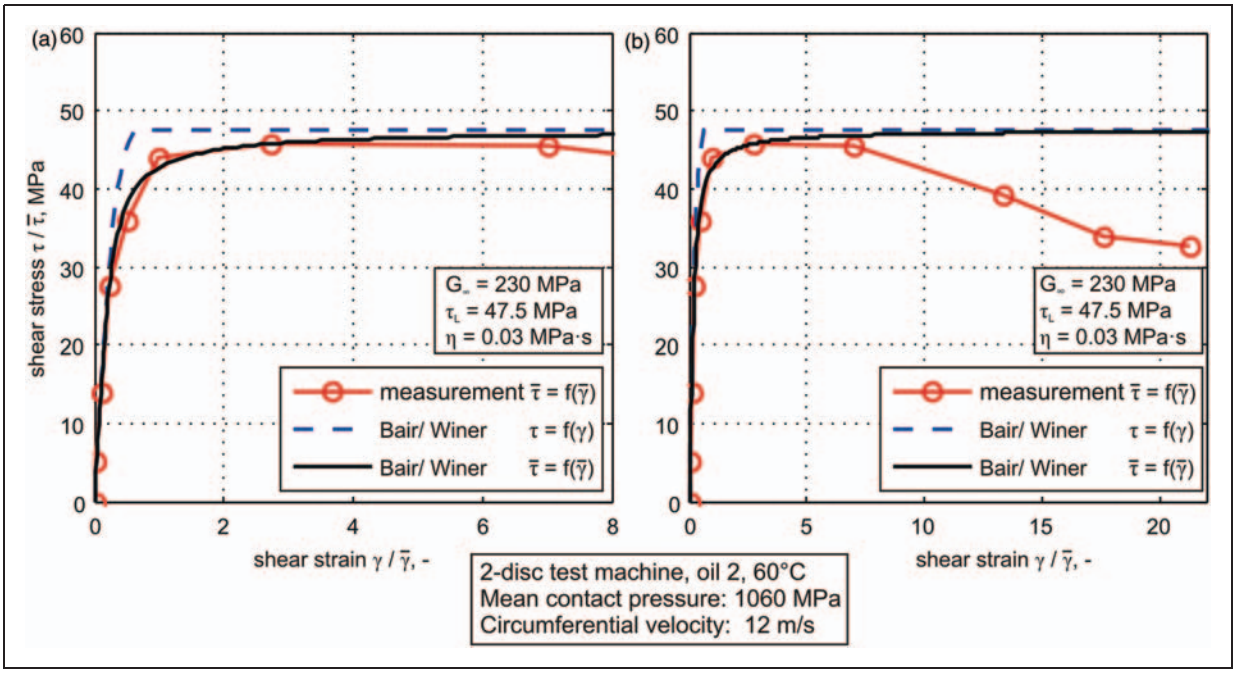

Figure 17. Comparison between experimental results and calculations of shear stress for mineral oil 2 by applying the Bair–Winer model against both shear and average shear strains at a rolling speed of 12 m/s in (a) vicinity of origin and (b) full range.

$$\bar{\gamma} = \frac{\bar{s}}{h_c} = \Delta v \cdot \frac{b}{v} \cdot \frac{1}{h_c} = \frac{S_L \cdot b}{h_c} \tag{12}$$

$$\dot{\bar{\gamma}} = \frac{\Delta v}{h_c} = \frac{S_L \cdot v}{h_c} \tag{13}$$

with

$$\Delta v = v_1 - v_2, \; v = \frac{v_1 + v_2}{2} \tag{14}$$

$$S_L = \frac{v_1 - v_2}{\frac{1}{2}(v_1 + v_2)} = \frac{\Delta v}{v} \tag{15}$$

Figure 13 explains the meaning of these expressions.

The central film thicknesses were calculated as shown before according to Hamrock[17] using the pressure viscosity coefficients determined for 200 MPa pressure. Additionally, the friction coefficients were transformed into mean shear stresses as explained earlier in this article. Subsequently, the average shear stresses were plotted against average shear strain (Figure 14) as well as against average shear rate (Figure 15). The purpose was to judge if the fluid is predominantly behaving elastic or viscous. Purely elastic behaviour would result in identical curves versus shear rate irrespective of speed, while purely viscous behaviour should yield identical curves versus shear rate.

None of the two methods of representation delivers identical slopes through the origin, indicating viscoelastic behaviour. With increasing rolling speed, the slopes versus shear rate decline. As we are in the nearly isothermal region, this should not simply be attributed to a thermal reduction of viscosity. However, an elastic contribution to shear would principally increase the apparent shear rate, especially at elevated rolling speeds as it then builds up during a shorter passage time through the contact. With decreasing rolling speed, the viscous shear rate becomes more dominant.

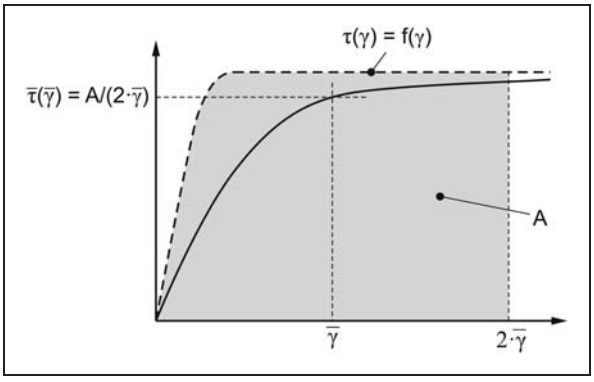

Figure 18. Transformation of the true shear vs. strain relationship for a fluid into the mean shear vs. mean strain relationship in a rolling contact.

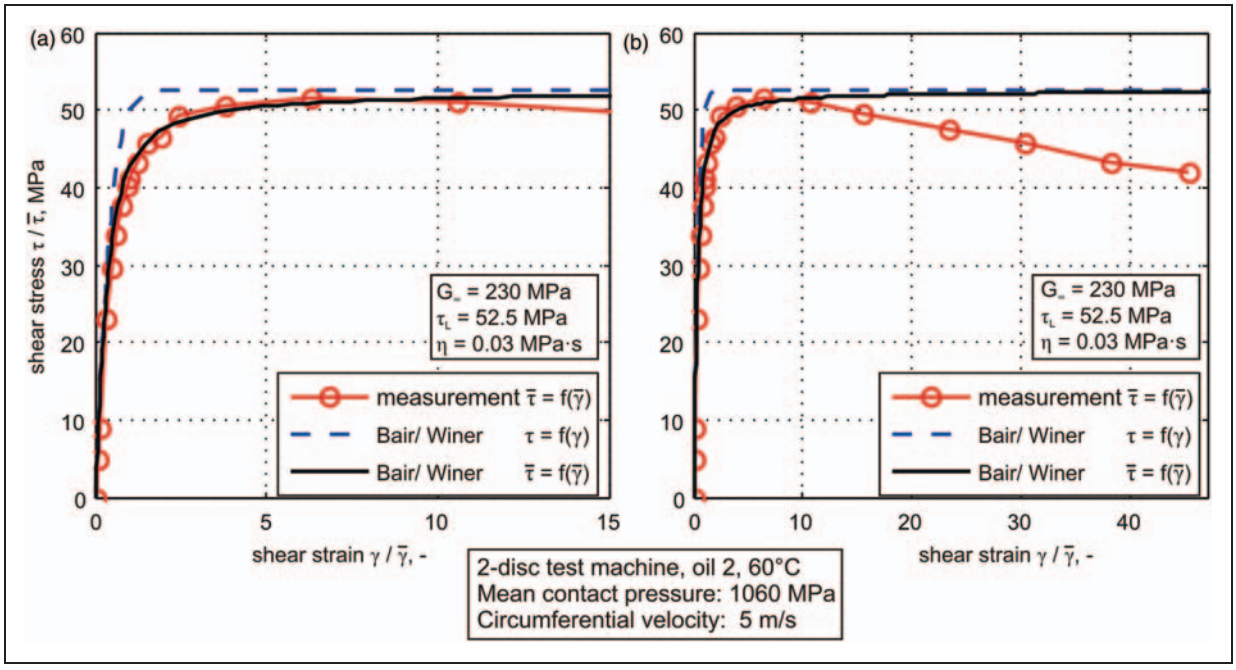

Figure 19. Comparison between experimental results and calculations of shear stress for mineral oil 2 by applying the Bair–Winer model against both shear and average shear strains at a rolling speed of 5 m/s in (a) vicinity of origin and (b) full range.

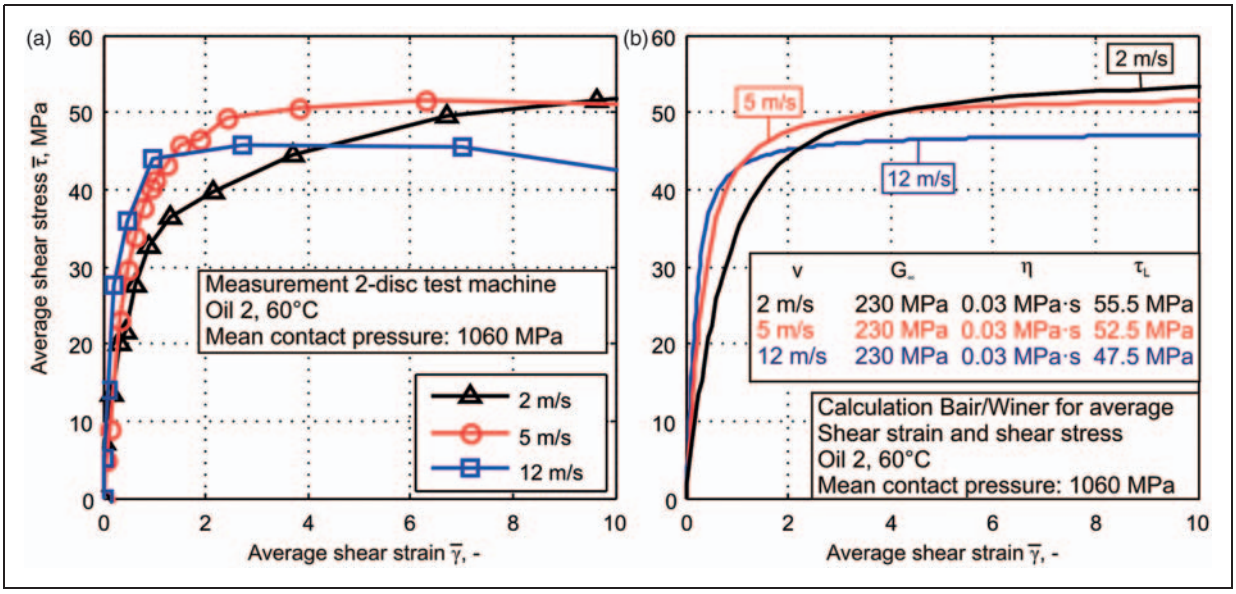

Figure 20. Comparison between experimental results and calculations based on the Bair–Winer model for mineral oil 2 at rolling speeds of 2, 5 and 12 m/s when plotted against the mean shear strain in the contact.

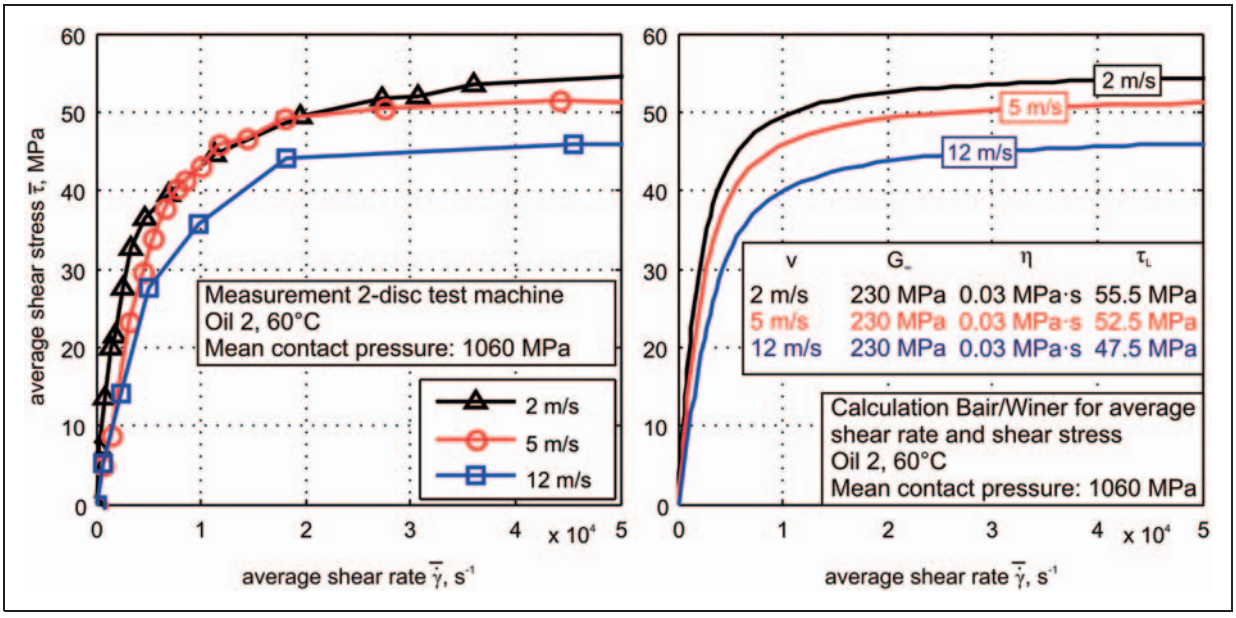

Figure 21. Comparison between experimental results and calculations based on the Bair–Winer model for mineral oil 2 at rolling speeds of 2, 5 and 12 m/s when plotted against the mean shear rate in the contact.

In contrast, when plotting against shear, the highest rolling speed delivers the steepest slope which should tend towards G_∞. With decreasing rolling speeds, the viscous relaxation becomes more and more prominent due to the extended passage times through the contact and hence the slope declines. An iterative approach to find the best fit to the measured slopes in the vicinity of the origin for all three rolling speeds investigated resulted in $G_\infty = 230$ MPa and $\eta = 0.03$ MPas.

From the initial slope at 12 m/s and Dyson's approximation of G_∞ as about four times τ_l,[7] a value around 230 MPa would indeed be a good estimate. However, according to laboratory measurements by different authors,[2,26–28] the real shear modulus should be much higher, up to more than 2 GPa. Also, the chosen viscosity is far below the range indicated by the extrapolation of laboratory measurements according to Tait–Doolittle. Therefore, as stated above, one should

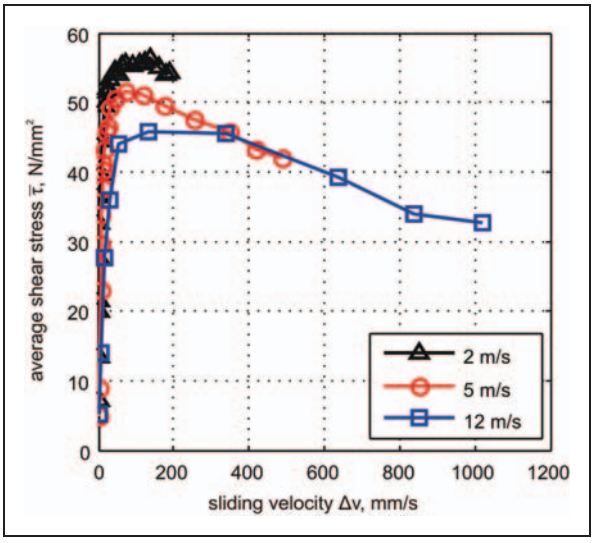

Figure 22. Experimental mean shear stresses against sliding velocity at rolling speeds of 2, 5 and 12 m/s.

be careful to interpret the selected set of parameters as true fluid properties. Shear thinning may well have a noticeable influence.

In a next step, identical values for shear modulus and viscosity were implemented into the Bair–Winer model for each speed together with τ_l values taken from Figure 7(a), that means, different for each speed. The results were treated like a constitutive model for the fluid and then applied to the rolling contact in the two-disc machine in an attempt to reproduce the measured traction curves.

With the selected parameter set, the Bair–Winer relation was able to reproduce the slope of all measured traction curves around the origin by setting γ equal to $\bar{\gamma}$, respectively τ equal to $\bar{\tau}$ in the contact (Figures 16, 17 and 19). With increasing shear, respectively, shear stresses the slopes of the measured curves become less steep and the limiting values τ_l are reached at larger shear values than with the formula. However, the formula is supposed to give the real relationship for the fluid which can be locally applied, whereas the measurements represent an averaged shear stress as a function of average shear in the contact. When defining $\bar{\gamma}$ as the shear in the middle of the contact, the minimum shear at the inlet will be 0 and the maximum shear at the outlet $2\bar{\gamma}$, if one assumes constant film thickness and relative tangential velocity throughout the contact (Figure 13). Therefore, the limiting shear stresses will not be reached at all points of the contact area at the same time. If the assumption of a sensible contribution of elastic shear strain would hold true for the entire contact, infinitely high slip values would be required to reach the limiting stress at the inlet to the contact, as shear strain always starts from zero and increases during the passage of the contact. As a first approximation, one may integrate τ over the interval from 0 to $2\bar{\gamma}$ in order to obtain the corresponding $\bar{\tau}$, in rolling contact (Figure 18)

$$\bar{\tau}(\bar{\gamma}) = \frac{1}{2\bar{\gamma}} \int_0^{2\bar{\gamma}} \tau(\gamma) \mathrm{d}\gamma \tag{16}$$

In this way, one obtains modified Bair–Winer curves for the rolling contact which match the measured values quite well, especially for 5 and 12 m/s, (Figures 16, 17, 19 and 20), where shear stresses are plotted versus shear strain. Obviously, as the same data are used, the same good match results when plotting the shear stresses against shear rate instead of shear strain (Figure 21). Because of frictional heating, the measured curves depart from the predicted ones at a frictional power of about 4 W/mm^2, while the theoretical isothermal curves continue to rise asymptotically to the assumed value of τ_l. When plotting traction curves with different rolling speeds and constant contact pressures instead of versus slip versus the mean relative or sliding velocity in the contact (Figure 22), the decline always appears to start around 100 mm/s and the curves will converge into one single function at elevated sliding speeds, underlining the thermal nature of this effect. At constant normal load, the sliding speed is a measure of the frictional power dissipated in the contact. For 2 m/s, a certain 'delay' of shear stress build-up with shear appears for the measured curves (Figure 16). At the beginning of the 'plateau', the shear stress values are comparable close to the ones obtained at higher rolling speeds and only with further increasing shear they continue to rise to their maximum. This may indicate a slight time dependency of the limiting shear stress; the time a fluid particle is spending under the high pressures in the contact is much longer with the lower speed and would therefore allow higher limiting shear stresses to develop.

It should be stressed again, though, that the nonlinear variations of limiting shear stress across the contact due to pressure and temperature variation are neglected in the simplified approach applied here and a more thorough analysis as in the study of Olver and Spikes[13] and Morgado et al.[29] needs to be performed.

Applications to rolling element bearings and toroidal drives

The results described above have already been successfully applied to two tribological systems.

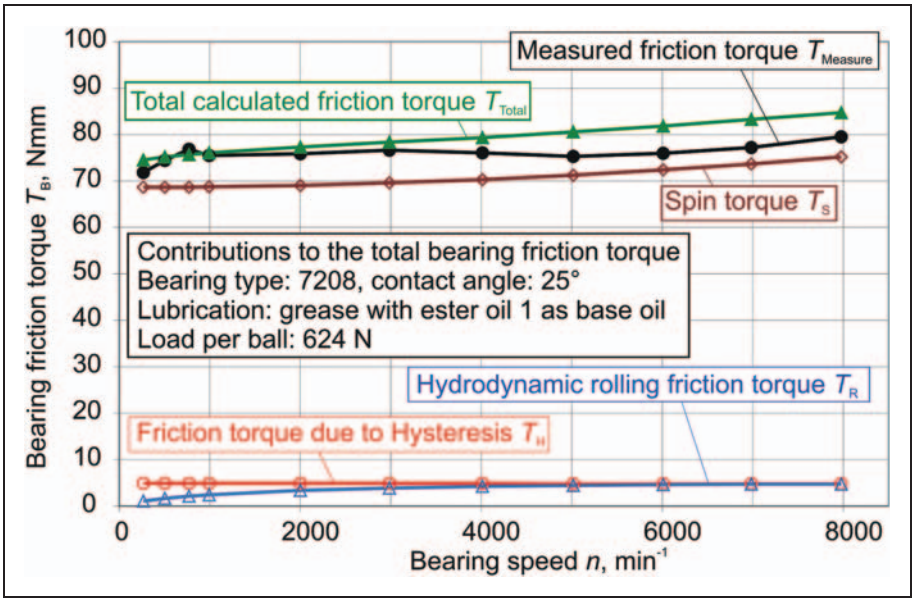

Figure 23. Contributions to frictional torque for an angular contact ball bearing grease lubricated with a barium complex thickener and ester oil I as base oil.[30]

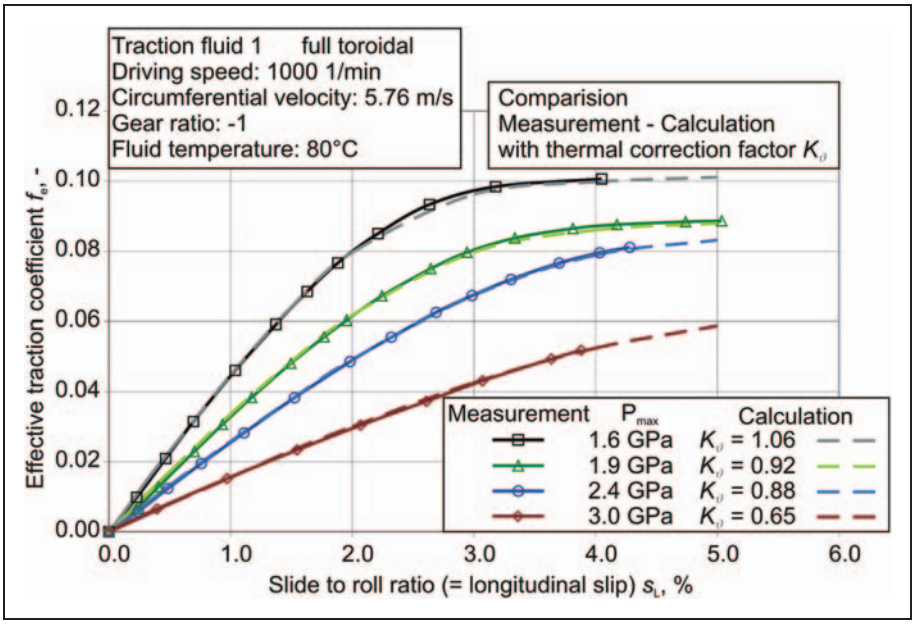

Figure 24. Measured and calculated traction/slip relationships for a full toroidal variator geometry.[3,4]

In case of angular contact ball bearings, spin substantially contributes to the overall bearing friction torque and hence, the traction characteristics of the lubricant are crucial. Figure 23 demonstrates the good correlation obtained with measurements using the limiting shear stress dependencies on pressure, temperature and speed described above. Due to the spin-to-roll ratios involved, the influence of viscoelastic fluid properties and of the elastic deformations of the contacting bodies is negligible in this example. The local limiting shear stresses in each point of the contact area are therefore determined and integrated to deliver the spin torque.

The same simplifying assumption was originally made for toroidal traction drives, while thermal correction factors were introduced to account for the frictional heating in the contacts due to the high amounts of spin and longitudinal slip. In case of a full toroidal variator spin-to-roll ratios are always in

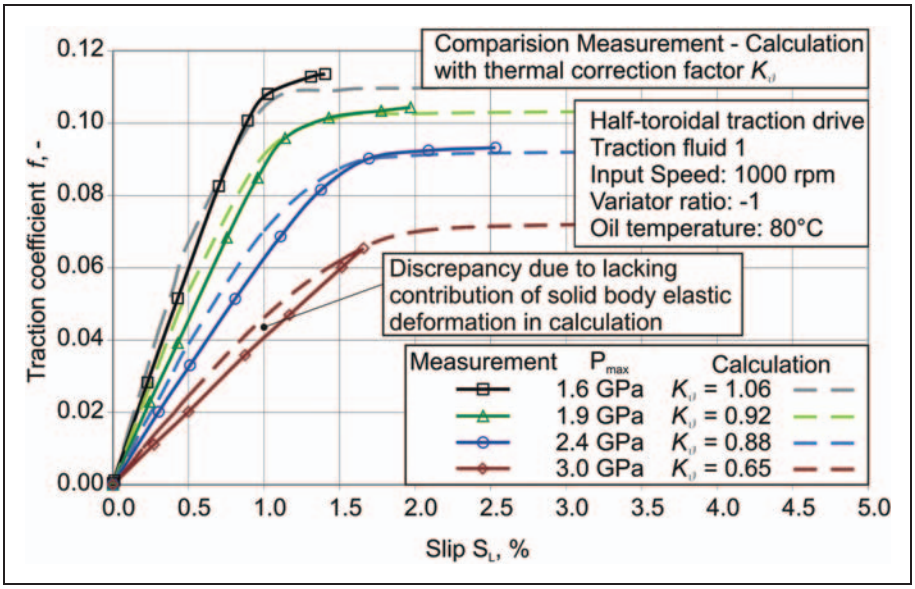

Figure 25. Measured and calculated traction/slip relationships for a half toroidal variator geometry as a function of maximum contact pressure.[3,4]

a range where the limiting shear stresses will be reached almost all over the contact area. Accordingly, a very good match with measurements is visible in Figure 24. However, half toroidal variators work with considerably less spin and, therefore, deviations between measurements and simplified calculations appear in Figure 25. When considering the elastic slip values contributed by the rolling elements in Figure 12, these may well serve as an explanation for those discrepancies and, therefore, need to be included.

Conclusions

The evaluation of two-disc roller test traction data presented in this article strongly supports the concept of a Mohr–Coulomb-type limiting shear stress in elastohydrodynamic lubrication contacts. At least, there is no evidence against it. A more complete picture is expected from the continuation of the work of Jacobson[16] with the high pressure rheometer at Lund University currently under way.

The influence of various parameters on the assumed limiting shear stress was studied in detail with results deserving further investigations. It could also be demonstrated that the limiting shear stress characteristics dominate friction in angular contact ball bearings and traction drives and that computations based thereupon will deliver realistic results. When properly accounting for the elastic compliance of the contacting solid bodies, using viscosity and elastic shear modulus as fitting parameters and applying the correct limiting shear stress, the Bair–Winer model is able to correctly approximate measured traction curves over a wide range of rolling speeds with one identical fitting parameter set. This approach is acceptable for practical purposes; however, it is doubtful if the fitted values of viscosity and elastic modulus represent the real properties of the fluid. Instead of averaging, it would be more realistic to base computations on the local properties of the fluid film in the contact area including a physically correct modelling of shear thinning. This has already been successfully attempted.[31] A next step should consist in including the mixed lubrication regime and to compute local shear stresses based on the real pressure distribution due to roughness.

Funding

This study was supported in part by the Arbeitsgemeinschaft industrieller Forschungsvereinigungen 'Otto von Guericke' e.V. (AiF) and by the Forschungsvereinigung Antriebstechnik e.V. (FVA).

Acknowledgements

The authors wish to thank S. Bair and B. Jacobson for ongoing discussions which have substantially contributed to this study. Finally, we thank Professor H. Schwarze and Dr.-Ing. L. Brouwer from the Technical University of Clausthal for the high-pressure viscosity measurements and Dr Th. Elfrath for the kind permission to use the ball on disc apparatus at Volkswagen AG.

References

1. Bair S and Kotzalas M. The contribution of roller compliance to elastohydrodynamic traction. *STLE Tribol Trans* 2006; 49(2): 218–224.

2. Bair S. *High pressure rheology for quantitative elastohydrodynamics*. Tribology and Interface Engineering Series, No. 54. Amsterdam, The Netherlands: Elsevier, 2007.
3. Poll G and Meyer C. Rheology model for traction fluids used in toroidal traction drives. In: *Proceedings of the CVT-hybrid international conference*, Maastricht, Eindhoven University of Technology, Automotive Technology Centre, Eindhoven, The Netherlands, 17–19 November 2010, pp.61–66.
4. Meyer C. *Reibung in hoch belasteten EHD-Wälzkontakten*. PhD Thesis, Leibniz Universität Hannover, 2010.
5. Plint MA. Traction in elastohydrodynamic contacts. *Proc Instn Mech Engrs* 1967; 182(14, Pt. 1): 300–306.
6. Johnson KL and Cameron R. Shear behavior of elastohydrodynamic oil films at high rolling contact pressures. *Proc Instn Mech Engrs* 1967; 182(14, Pt. 1): 307–319.
7. Dyson A. Frictional traction and lubrication rheology in elastohydrodynamic lubrication. *Philos Trans R Soc London Ser A* 1970; 266: 1–33.
8. Eyring H. Viscosity, plasticity and diffusion as examples of reaction rates. *J Chem Phys* 1936; 4: 283–291.
9. Tevaarwerk JL and Johnson KL. Shear behaviour of elastohydrodynamic oil films. *Proc R Soc London Ser A* 1977; 356(1685): 215–236.
10. Bair S and Winer WO. The high shear stress rheology of liquid lubricants at pressures of 2 to 200 MPa. *ASME J Tribol* 1990; 112(2): 246–253.
11. Carter FJ. On the action of a locomotive driving wheel. *Proc R Soc London Ser A* 1926; 112: 151–157.
12. Poll G. *Der Einfluss der realen Systemeigenschaften auf die Kraftschlussgesetze bei wälzender Relativbewegung*. PhD Thesis, Rheinisch-Westfälische Technische Hochschule Aachen, 1983.
13. Olver AV and Spikes HA. Prediction of traction in elastohydrodynamic lubrication. *Proc IMechE Part J: J Engineering Tribology* 1998; 212: 321–332.
14. Tevaarwerk JL. Traction in lubricated contacts. In: *Proceedings of the contact mechanics and wear of rail/wheel systems*, Vancouver, Canada, 6–9 July 1982, pp.121–132. Waterloo, Canada: University of Waterloo Press.
15. Evans CR and Johnson KL. The rheological properties of elastohydrodynamic lubricants. *Proc IMechE Part C: J Mechanical Engineering Science* 1986; 200(5): 303–312.
16. Jacobson BO. High-pressure chamber measurements. *Proc IMechE Part J: J Engineering Tribology* 2006; 220(3): 199–206.
17. Hamrock BJ. *Fundamentals of fluid film lubrication*, 2nd ed. New York: Dekker, 2004.
18. Bode B. Entwicklung eines Quarzviskosimeters für Messungen bei hohen Drücken. TU Clausthal, Tribologie und Schmierungstechnik, 35. Jahrgang, Heft 5, 1988.
19. Hirschfelder JO, Curtiss CF and Bird RB. *Molecular theory of gases and liquids*. New York: Wiley, 1954, p.261.
20. Doolittle AK. Studies in Newtonian flow. II. The dependence of viscosity of liquids on free space. *J Appl Phys* 1951; 22(12): 1471–1475.
21. Barus C. Isothermals, isopiestics and isometrics relative to viscosity. *Am J Sci* 1893; 45(266): 87–96.
22. Walbeck T. Das *Viskositätsverhalten und die Schmierfilmbildung von Schmierstoffen in Abhängigkeit von Druck und Temperatur*. PhD Thesis, Technische Hochschule Aachen, 2004.
23. Bowden PB. The yield behavior of glassy polymers. In: RN Haward (ed.) *The physics of glassy polymers*. New York, NY: Halstead Press, 1973, pp.279–339.
24. Bair S and McCabe C. A study of mechanical shear bands in liquids at high pressure. *Tribol Int* 2004; 37: 783–789.
25. Carreau PJ. Rheological equations from molecular network theories. *Trans Soc Rheol* 1972; 16(1): 99–127.
26. Hutton JF and Philips MC. Shear modulus of liquids at elastohydrodynamic pressures. *Nat Phys Sci* 1972; 238: 141–142.
27. Barlow AJ, Harrison G, Irving JB, et al. The effect of pressure on the viscoelastic properties of liquids. *Proc R Soc London Ser A* 1972; 327: 403–412.
28. Hutton JF. Reassessment of rheological properties of LVI 260. *ASME J Lubr Technol* 1984; 106: 536–537.
29. Morgado PL, Otero JE, Muñoz Sanz JL, et al. Models for predicting friction coefficient and parameters with influence in elastohydrodynamic lubrication. *Proc IMechE Part J: J Engineering Tribology* 2009; 223: 949–958.
30. Poll G, Wang D and Neubauer T. Wälzlager-Reibmomente unter Berücksichtigung der Schmierstoff-Rheologie und Versorgung. In: *Gleit- und Wälzlagerungen*. Düsseldorf: VDI-Verlag GmbH, 2011, VDI-Bericht, No. 2147, pp.125–146.
31. Habchi W, Vergne P, Bair S, et al. Influence of pressure and temperature dependence of thermal properties of a lubricant on the behaviour of circular TEHD contacts. *Tribol Int* 2010; 43: 1842–1850.

Appendix

Notation

a	semi-major axis of the Hertzian contact ellipse
A	area
b	semi-minor axis of the Hertzian contact ellipse
f	friction coefficient
f_C	Coulomb friction coefficient
$f_{\max}$	limiting friction coefficient
F_N	normal force
F_t	traction force
G	elastic shear modulus of a solid
G_∞	limiting elastic shear modulus of a fluid
h_c	central lubricant film thickness
K_θ	thermal correction factor
p	contact pressure
$\bar{p}$	mean contact pressure
$p_{\max}$	maximum pressure

R_a	centreline averaged roughness	$\bar{\gamma}$	average shear strain
s	displacement	$\dot{\gamma}$	shear rate
S_L	slide-to-roll ratio	$\bar{\dot{\gamma}}$	average shear rate
t	time	ε	elastic strain
T	torque	η	dynamic viscosity
v	rolling velocity	η_0	dynamic viscosity at atmospheric pressure
z	dimension z-axis	θ	temperature
		λ	film thickness parameter
$\alpha_{p,2000}$	viscosity pressure coefficient at 2000 bar	ν	Poisson's ratio
γ	shear strain	σ	root mean square roughness
$\gamma_{elastic}$	elastic shear strain in Maxwell model of an elastic-visco fluid	τ	shear stress
		$\bar{\tau}$	average shear stress
$\gamma_{viscous}$	viscous shear strain in Maxwell model of an elastic-visco fluid	τ_0	Eyring shear stress
		τ_L	limiting shear stress
γ_{total}	total shear strain in Maxwell model of an elastic-visco fluid	$\bar{\tau}_L$	average limiting shear stress
		φ	angle